Chapter 4

DFT based study on the mechanism of an unexpected reaction of aldehydes with 1, 3-dicarbonyl compounds

In this chapter we have investigated the mechanism of an unexpected reaction between two molecules of 1, 3-dicarbonyl compound and one molecule of the aldehyde in presence of molecular iodine by density functional theory based approach. The geometries and the frequencies of reactants, intermediates and transition states are calculated using Becke three parameter exchange and Lee-Yang-Parr correlation functional. The vibrational analysis, intrinsic reaction coordinate (IRC) calculation and ESP analysis verify the authenticity of the transition states. Depending on substitution pattern of 1, 3-dicarbonyl compound, there may be two pathways, one leads to furan derivative and the other to cyclopropane derivative. The nucleus independent chemical shift (NICS) values have been calculated for the intermediates, products and the corresponding transition states to ensure the aromaticity contribution to the reaction pathway. The results are in good agreement with the experimental findings.

4.1 Introduction

Cyclopropane ring is found both in natural products and in biologically active mole-cules.[1-5] The unusual bonding and ring strain make it an interesting moiety to organic and bioorganic chemists. It can easily undergo selective ring opening and [1, 2] cycloaddition reactions. A variety of cyclopropanation reactions are well documented.[6] The substituted dihydrofurans, an important class of heterocycles are widely present in numerous natural products and show antibacterial as well as antifungal activities.[7-13] Due to diverse roles in organic synthesis, the synthetic methodologies for dihydrofurans have also been studied in detail.[6a, 14]

Oxidative addition reaction of various aldehydes with 5,5-dimethylcyclohexane-1,3-dione and 1,3-indandione can selectively endow with spiro dihydrofuran and cyclopropane derivatives in presence of iodine and dimethylaminopyridine (DMAP).[6a] It is a solvent free reaction and reported to be an unexpected reaction. Generally 1, 3-dicarbonyl compound reacts with an aldehyde and gives aldol condensation product. However, in this case as iodine and DMAP are introduced, this reaction proceeds to further cyclization following an unusual pathway.

The mechanism of aldol condensation reactions has already been studied extensively.[15-20] Bouillon et.al have studied diastereoselective intramolecular aldol condensations of 1,6-diketones in ab initio method.[16] Arno and Domingo have studied proline catalyzed aldol reaction between acetone and isobutyraldehyde.[17] However, no such mechanistic study has been reported for the title reaction. So our present work aims to investigate the most plausible mechanistic pathway in DFT framework which will be beneficial to further theoretical and experimental studies. To understand the mechanism of this highly selective cyclization, we have theoretically investigated the common steps of the reaction with acetyl acetone as 1, 3-dicarbonyl compound and acetaldehyde. To study the step of cyclization, we have taken (1) dimedone and 3- nitro benzaldehyde in one plausible path and (2) 1,3-indanedione and 3-nitro benzaldehyde in another (Scheme 4.1).

4.2 Methodology

In this work, we explore mechanistic pathways for this unexpected reaction through DFT studies using Becke three parameter exchange and Lee-Yang-Parr correlation functional. Since the systems investigated in this work are quite large, the geometries of all the reactants, intermediates, transition states and products have been optimized using the simplest split-valence basis function for computational economy. As iodine is undefined in this standard basis set, LANL2DZ is used as an extrabasis function for iodine. For all optimized structures, frequency analysis has been carried out. This allows one to assign the reactants and products as genuine minima and shows one imaginary frequency for the transition states. Intrinsic reaction coordinate (IRC) calculations have been done to verify whether the transition states connect the reactants to the products. The exchange correlation functional, which is used in this work, contains spurious electron self interaction, related to long range nondynamic correlation of electron.[21] The self interaction error (SIE) influences the shape of the potential energy surface near the transition state by lowering the barrier height.[22] Being aware of this fact, we have further refined our B3LYP results by carrying out single point calculation at MP2 level on the transition states.[23] Reactivity of any molecule at a specific site can be determined by local reactivity parameters such as Fukui function and so on. In this study, we have calculated Fukui function at different sites of a molecule. Regioselectivity for nucleophilic or electrophilic attack at site k can be ascertained through evaluation of Fukui function (f_k^i), [24-26] and can be estimated using population analysis as

$$f_k^+ = [\rho_k(N+1) - \rho_k(N)] \quad \text{for nucleophilic attack} \tag{4.1}$$

$$f_k^- = [\rho_k(N) - \rho_k(N-1)] \quad \text{for eletrophilic attack} \tag{4.2}$$

where $\rho(N+1)$, $\rho(N)$ and $\rho(N-1)$ are the electron densities of the (N+1), N and (N−1) electron systems respectively.[27, 28] Condensed form of these functions was presented by Yang and Mortier[29] yielding

$$f_k^+ = [q_k(N+1) - q_k(N)]\,, \tag{4.3}$$

$$f_k^- = [q_k(N) - q_k(N-1)\,], \tag{4.4}$$

where $q_k(N+1)$, $q_k(N)$, $q_k(N-1)$ are the charges at atom *k* on the anion, neutral, and cation species obtained by different population analysis. Since here we do not use any diffused function, Mulliken population analysis (MPA) has been used to estimate the condensed Fukui function. In this work Fukui functions are calculated following Eqs. (4.3) and (4.4). The thermodynamic functions (ΔG and ΔH) are calculated within ideal gas, rigid-rotor and harmonic oscillator approximations at 298.15K temperature and 1 atm pressure. The nucleus independent chemical shift (NICS) is a useful tool to analyze the contribution of aromaticity to the reaction path.[30-34] We have calculated the NICS values for the intermediates, products and also for the transition states to ensure the σ [NICS(0)] and π [NICS(1)] aromaticity contribution to the reaction path.

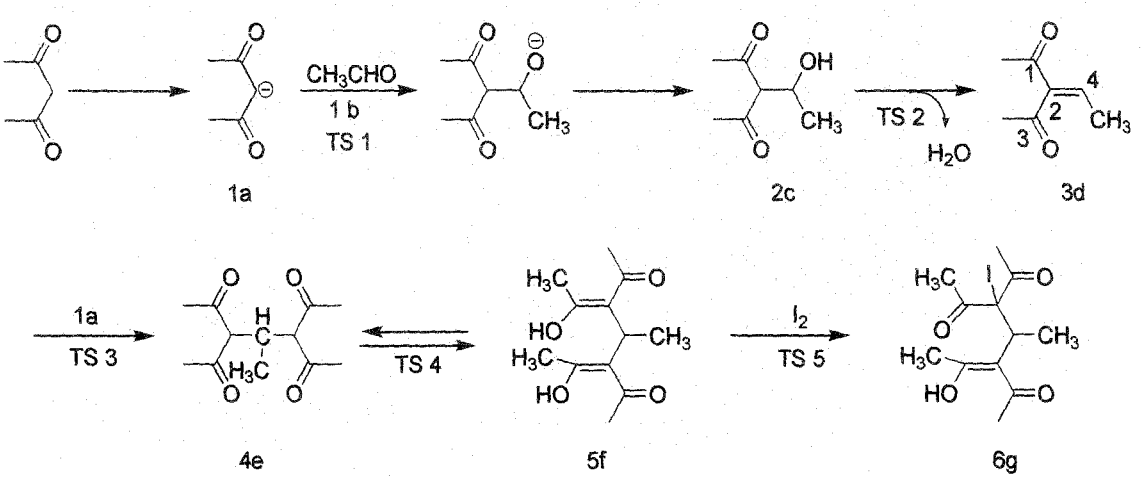

(A)

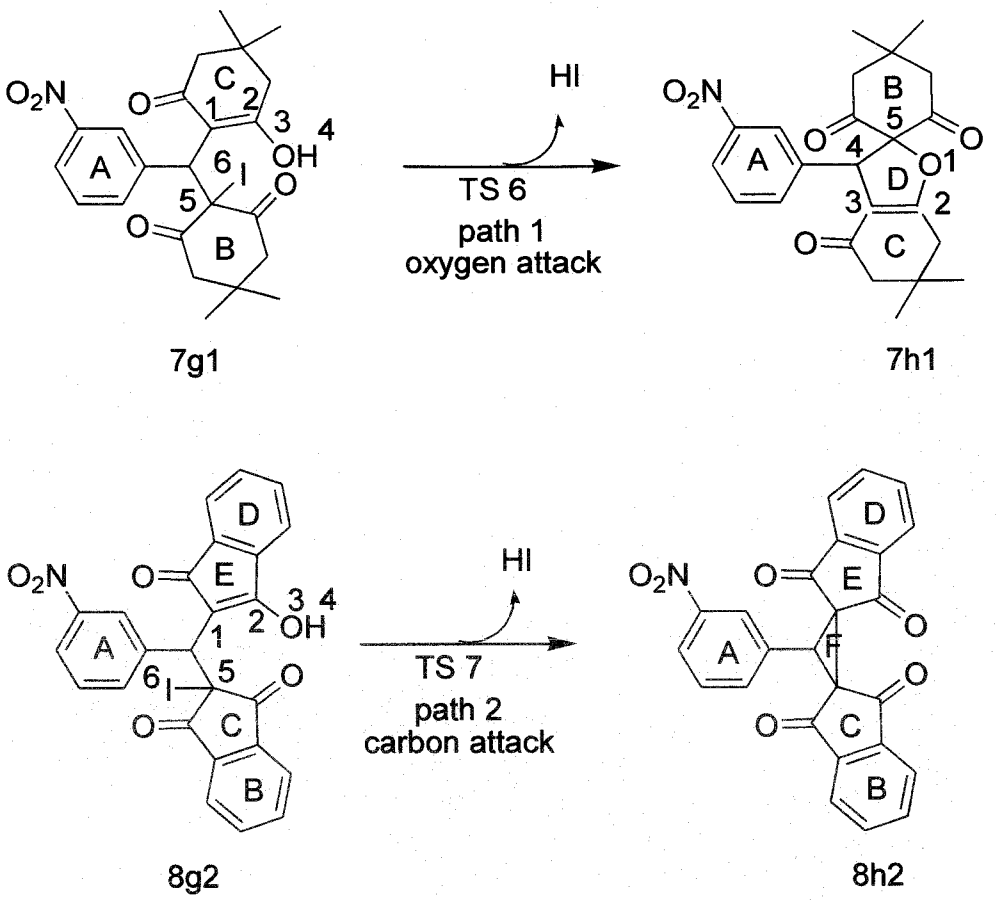

(B)

Scheme 4.1: (A) Schematic mechanism for the general steps of the reaction. (B) Two possible paths of cyclization; $7g_1$ is formed in the reaction between dimedone and 3-nitro benzaldehyde and $8g_2$ is formed in the reaction between 1,3-indanedione and 3-nitro benzaldehyde which on subsequent cyclization form $7h_1$ and $8h_2$ respectively.

4.3 Results and discussion

In this work, we have investigated the reaction mechanism using exchange-correlation functional B3LYP in the unrestricted DFT formalism. All structures are optimized using 3-21G basis function. LANL2DZ is used as an extrabasis function for iodine. All calculations are implemented through Gaussian 03W quantum chemical

package.[35] The potential energy map for the pathways related to the reaction between two molecules of the 1,3-dicarbonyl compound and one molecule of the aldehyde in presence of molecular iodine in basic medium is illustrated in Figure 4.1 where the relative energies in the parenthesis are taken from Table 4.1.

Our investigation shows that 1,3 dicarbonyl compound produces a carbanion (1a) in alkaline medium (Scheme 4.1). Now the carbanion (1a) undergoes nucleophilic attack to an aldehyde (1b) and gives the aldol condensation product (2c) via the transition state (TS1). The unique imaginary frequency of TS1 is -62.44 cm^{-1} and therefore it can be affirmed as the real one. This reaction is a barrier less exothermic reaction having $\Delta H=-1534.695$ kJ mol^{-1}. The spontaneity of this step is also apparent from the negative ΔG value (Table 4.2). Subsequent elimination of water from (2c) gives the product (3d) through TS2 which shows an imaginary frequency -1249.34 cm^{-1} originating from oscillation of the acidic proton from carbon to –OH group. This step of the reaction is slightly endothermic in nature ($\Delta H=117.661$ kJ mol^{-1}) and requires an activation energy of 195.300 kJ mol^{-1}. Electrophilicity of carbon centers in (3d) is quantified in terms of condensed Fukui functions (Table 4.3). Higher the value of Fukui function (f_k^+), greater is the probability of nucleophilic attack at site *k*. Now the carbanion (1a) produced from the second molecule of 1, 3 dicarbonyl compound reacts with double bonded C attached with –Me group of (3d) as predicted from Fukui functions via the transition state TS3 and 1,4 Michael addition takes place. Before the transition state can be achieved an intermediate (IM_2) is formed by the weak vanderwaals interaction. Frequency calculation of TS3 shows an imaginary frequency -255.26 cm^{-1} leading towards the product (4e). This step of reaction requires small activation barrier of 46.988 kJ mol^{-1}. Therefore it is expected to be fast. This is also supported by negative ΔG value (-1526.653 kJ mol^{-1}). Thermochemical analysis shows that this step is highly exothermic (Table 4.2) in nature. The compound (4e) undergoes enolization with an activation barrier of 294.981 kJ mol^{-1}. Here we have observed that the keto form (4e) is energetically lower than the corresponding enol form (5f). The tautomerism takes place through a four membered transition state (TS4) (Figure 4.2) which shows an imaginary frequency -1732.10 cm^{-1} originating from the oscillation of proton from carbon to carbonyl oxygen. In this context one can note that the tautomeric process is endothermic in nature. The enol form (5f)

which seems to be an intermediate, undergoes iodination at the most activated site to give the key intermediate (6g) via TS5 which is a six membered transition state (Figure 4.2) having an imaginary frequency −176.90 cm^{-1}. This step requires activation energy of 1302.609 kJ mol^{-1}. Nonetheless according to thermochemical analysis, this step is slightly exothermic in nature.

Table 4.1

Theoretical prediction of total energy (Hartree) at MP2, ZPVE (Hartree/particle) and relative energies ΔE (a.u) for reactants, products, intermediates and transition states.

Species	Total energy		ZPVE	ΔE (a.u)
	UB3LYP	MP2		
1a+1b	-496.284	-494.099	0.166	0.0
IM1	-496.322	-494.300	0.169	-0.032
TS1	-496.270	-494.252	0.169	0.016
2c	-496.889	-494.883	0.184	-0.6
TS2	-496.814	-494.795	0.179	-0.517
3d+H_2O	-496.839	-494.660	0.177	-0.561
3d+1a	-764.170	-760.765	0.267	-266.666
IM2	-764.217	-761.076	0.270	-266.707
TS3	-764.199	-761.068	0.270	-266.699
4e	-764.795	-761.681	0.285	-267.297
TS4	-764.682	-761.552	0.279	-267.174
5f	-764.797	-761.613	0.285	-267.229
5f+ I_2	-14546.340	-14537.359	0.285	-14043.141
TS5	-14545.841	-14535.624	0.283	-14041.408
6g+HI	-14546.279	-14537.774	0.278	-14043.563
7g1	-8281.182	-8272.880	0.464	--
TS6	-8280.921	-8272.779	0.454	--
7h1+HI	-8281.172	-8272.860	0.452	--
8g2	-8349.764	-8341.350	0.342	--
TS7	-8349.485	-8341.260	0.330	--
8h2+HI	-8349.710	-8341.295	0.326	--

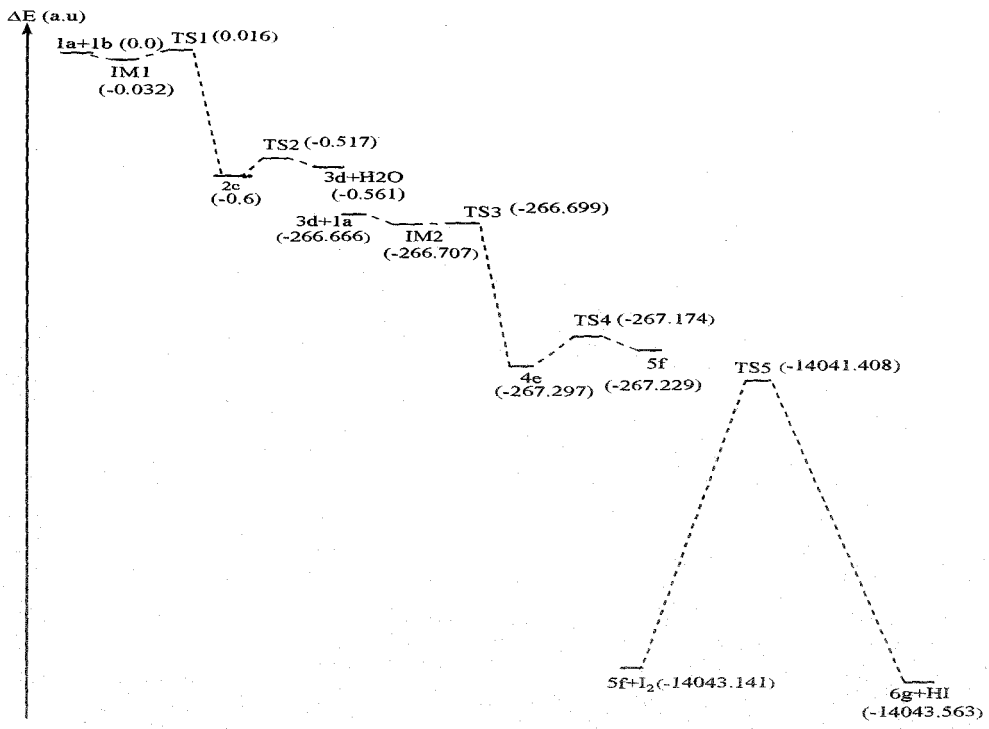
ΔE (a.u)
1a+1b (0.0)
TS1 (0.016)
IM1
(-0.032)
TS2 (-0.517)
2c
(-0.6)
3d+H2O
(-0.561)
3d+1a
(-266.666)
TS3 (-266.699)
IM2
(-266.707)
TS4 (-267.174)
4e
(-267.297)
5f
(-267.229)
TS5 (-14041.408)
5f+I2(-14043.141)
6g+HI
(-14043.563)

(A)

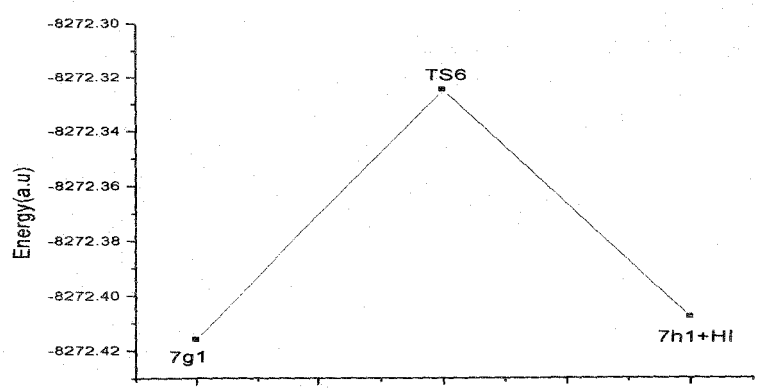
-8272.30
-8272.32
-8272.34
-8272.36
-8272.38
-8272.40
-8272.42
Energy(a.u)
TS6
7g1
7h1+HI

(B)

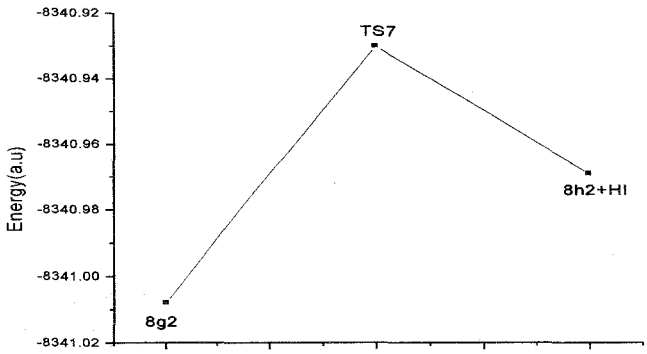

(C)

Figure 4.1 (A) shows the schematic representation of the energy profile (reactants, intermediates, transition states and products) for the general steps of the reaction [Scheme 4.1:(A)]. Whereas (B) and (C) show that of two cyclization pathways [Scheme 4.1: (B)].

Table 4.2

Free energy and enthalpy change of the reactions.

Conversion	$\Delta G(kJ\ mol^{-1})$	$\Delta H(kJ\ mol^{-1})$
1a + 1b → 2c	−1478.460	−1534.695
2c →3d	70.304	117.661
1a + 3d → 4e	−1526.653	−1584.673
4e → 5f	148.337	146.037
5f → 6g	−2.513	−9.585
$7g_1 \rightarrow 7h_1$	−34.765	8.149
$8g_2 \rightarrow 8h_2$	72.788	121.509

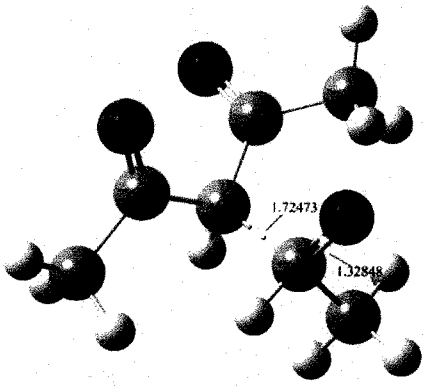

TS1

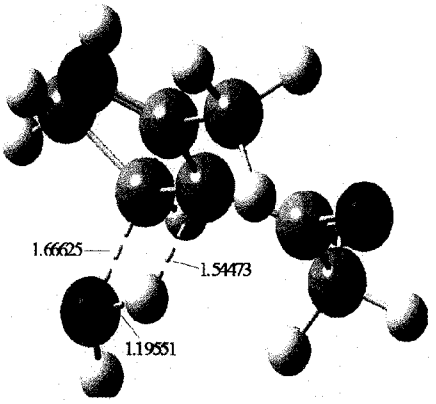

TS2

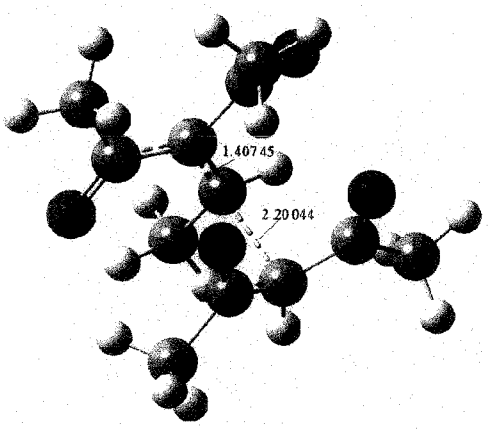

TS 3

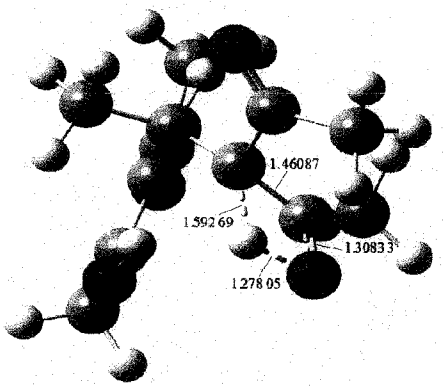

TS4

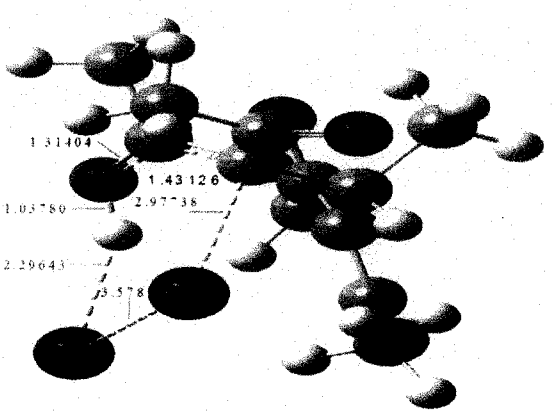

TS5

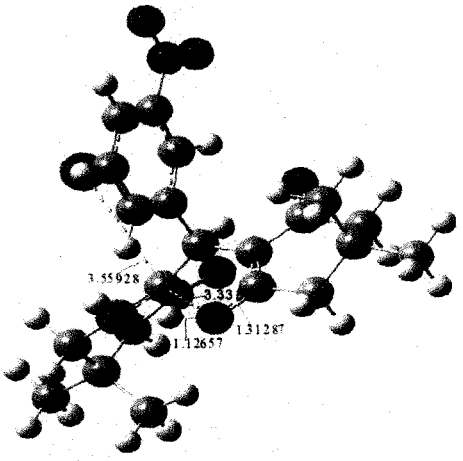

TS6

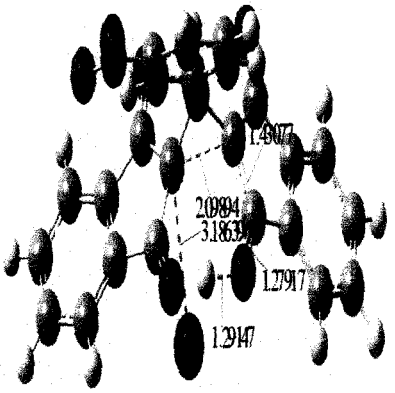

TS7

Figure 4.2 The optimized structures of the transition states corresponding to scheme 1. Distances are given in angstrom.

Table 4.3

Condensed Fukui functions at different probable positions of 3d for nucleophilic attack.

position	Condensed Fukui function
1-C	0.062
2-C	0.014
3-C	0.062
4-C	0.095

The discussion about the complication of the reaction mechanism is due here. The intermediate (6g) can undergo cyclization in two different ways (path 1 and path 2) which depends on the substitution pattern. In path 1, an intramolecular nucleophilic O-attack with an elimination of HI yields dihydrofuran. On the other hand, in path 2 a nucleophilic C-attack produces cyclopropane with an elimination of HI. To study two alternative pathways we have selected two different sets of reactants as shown in scheme 4.1(B). Reaction between dimedone and 3-nitro benzaldehyde goes via the first path i.e., the nucleophilic attack of oxygen which results dihydrofuran derivative and the corresponding transition state (TS6) is characterized by its negative frequency −237.73 cm^{-1}. Condensed Fukui function (f_k^-) calculation of intermediate $7g_1$ (Table 4.4) suggests

Table 4.4

Condensed Fukui functions at two different active sites of $7g_1$ and $8g_2$ for electrophilic attack.

Species	position	Condensed Fukui function
$7g_1$	1-C	0.013
	3-O	0.028
$8g_2$	1-C	0.082
	3-O	0.068

the higher electrophilicity of oxygen atom rather than carbon atom. Hence it can be predicted that the intermediate (7g1) must follow path 1. This prediction can be further supported by the analysis of electrostatic potential (ESP). The calculated electrostatic potential partial charges of the reacting sites of the intermediate ($7g_1$) and the transition state (TS6) are given in Table 4.5. There is some positive ESP charge on I atom in the intermediate whereas in the transition state it gains negative ESP charge. As the reaction proceeds from the intermediate to the transition state the negative ESP charge on C-5 atom shrinks and it is strewn on the I atom so that the I atom can be eliminated as I^- leaving C-5 as a site for nucleophilic attack. Increase of ESP charge (from 0.436 to 0.447) on hydrogen atom of –OH in the transition state (TS6) indicates the liberation of proton. The authenticity of the transition state (TS6) is thus justified by ESP analysis and the mechanism of this step is well understood. This step of the reaction requires an activation barrier of 680.747 kJ mol^{-1} and it is impulsive in nature (ΔG =–34.765 kJ mol^{-1}).

Table 4.5

ESP partial atomic charges of 7g1 and TS6 computed at the UB3LYP level.

Atom[a]	Partial atomic charges	
	7g1	TS6
C1	−0.460	−0.546
O3	−0.546	−0.534
H4	0.436	0.447
C5	−1.255	−0.816
I6	0.165	−0.014

[a] The atomic numbering system is shown in scheme 4.1.

However, in case of the reaction between 1, 3-indanedione and 3-nitro benzaldehyde the alternative path is followed; i.e., reaction takes place through C-attack. In this case the reaction proceeds through the transition state, TS7 (imaginary frequency $-230.84\ cm^{-1}$). Condensed Fukui function (f_k^-) has been calculated for the intermediate $8g_2$ (Table 4.4) which indicates higher susceptibility of electrophilic attack at carbon atom rather than oxygen atom. So the involvement of path 2 for the second case is well supported and predicted. This prophecy is further justified by ESP analysis. There is negative ESP charge on C-5 in the intermediate ($8g_2$) but it gains positive ESP charge (+0.051) in the transition state (Table 4.6). Positive ESP charge on hydrogen atom of OH increases from +0.442 to +0.505 in the transition state and iodine gains negative ESP charge (−0.321) in the transition state. This indicates liberation of proton and iodide ion in the form of HI. So the reaction proceeds in the right direction through this transition state (TS7) i.e., the authenticity of the transition state as well as the mechanism of this step are established by ESP analysis. This step of cyclization requires an activation energy of 728.312 kJ mol^{-1} and it is slightly endothermic (ΔH=121.509 kJ mol^{-1}) in nature.

Table 4.6

ESP partial atomic charges of 8g2 and TS7 computed at the UB3LYP level.

Atom[b]	Partial atomic charges	
	8g2	TS7
C1	−1.245	−0.236
C2	0.550	0.632
O3	−0.576	−0.558
H4	0.442	0.505
C5	−0.821	0.051
I6	0.130	−0.321

[b] The atomic numbering system is shown in scheme 4.1.

For the last two alternating steps we have calculated the nucleus independent chemical shift (NICS) of the intermediates, transition states and products (Table 4.7 and

Table 4.8) to establish the feasibility of the reaction. If we consider the first path (path 1), in the intermediate (7g1) all the rings are seen to be aromatic in nature [negative NICS(0) and NICS(1)]. Now when the intermediate (7g1) undergoes cyclization via TS6 an additional ring (D) is formed. In the transition state NICS(0) and NICS(1) values of the new ring (D) are found to be negative. For ring D, NICS(1) value is smaller than NICS(0) and both values increase in the product (7h1). Now for the second path of cyclization (path 2), the intermediate (8g2) possesses four aromatic rings. In the transition state (TS7) an additional ring (F) is being formed which is extremely aromatic in nature [NICS(0) value −35.56]. Both values [NICS(0) & NICS(1)] of ring (F) increase in the product (8h2). So the driving force of these two pathways is obviously the huge gain in aromaticity. Indeed this argument lends a strong support for this so-called unusual reaction.

Table 4.7

NICS(0) and NICS(1) values of 7g1, TS6 and 7h1 computed at the UB3LYP level.

	7g1		TS6		7h1	
Ring	NICS(0)	NICS(1)	NICS(0)	NICS(1)	NICS(0)	NICS(1)
A	−8.51	−10.72	−6.56	−8.40	−9.00	−10.96
B	−0.42	−1.29	0.26	0.07	−1.09	−3.10
C	−1.32	−1.53	0.86	−2.69	−1.32	−1.54
D	--	--	−2.88	−0.32	−5.10	−1.49
$NICS_{Total}$	−10.25	−13.54	−8.32	−11.34	−16.51	−17.09

Table 4.8

NICS(0) and NICS(1) values of 8g2, TS7 and 8h2 computed at the UB3LYP level.

	8g2		TS7		8h2	
Ring	NICS(0)	NICS(I)	NICS(0)	NICS(I)	NICS(0)	NICS(I)
A	−9.34	−10.94	−8.80	−10.87	−8.61	−10.55
B	−7.45	−10.83	−6.31	−9.33	−7.6	−10.49
C	3.90	−3.28	5.78	−0.78	5.78	−1.21
D	−6.24	−9.15	−6.65	−8.97	−7.54	−10.61
E	6.60	0.87	4.58	−0.85	5.66	−0.96
F	--	--	−36.25	−4.77	−35.56	−6.11
$NICS_{Total}$	−12.53	−33.33	−47.65	−35.57	−47.87	−39.93

As the applied functional is reported to be inadequate in producing an accurate picture of potential energy surface, [21-23] the results have been compared with single point MP2 calculations on B3LYP optimized geometries. MP2 energies of the reactants, transition states and products reproduce the energy ordering of DFT functional but with an overall scaled down representation. Comparison of DFT and post Hartee-Fock results are given in Table 4.1.

4.4 Summary

In this work we have studied the addition mechanism of two molecules of 1, 3-dicarbonyl compound and one molecule of aldehyde in presence of molecular iodine within unrestricted DFT framework using B3LYP hybrid functional. General steps of the reaction are studied using acetyl acetone as 1, 3-dicarbonyl compound and acetaldehyde. There may be two pathways depending on the substitution pattern of 1, 3-dicarbonyl compound. One leads to spiro dihydrofuran and other cyclopropane derivatives. Paths being followed in either situation can be predicted by condensed Fukui function calculation and by ESP analysis. In each steps transition states are calculated. Vibrational analysis, IRC calculations and ESP analysis confirm these transition states. The nucleus independent chemical shift (NICS) calculation suggests that the gain in aromaticity plays an important role in the last step of the reaction. Thermochemical analysis is in good agreement with each step of the proposed mechanism. As a whole, the present DFT study explains well the experimental finding and also provides the details of the reaction mechanism.

4.5.1 References and notes

1. Salaun, J.; Baird, M. S. *Curr. Med. Chem.*, **1995**, *2*, 511.
2. Lin, H. W.; Walsh, C. T. *The Chemistry of the Cyclopropyl Group*; (Ed. Rappoport, Z.) John Willey and Sons Ltd., New York, **1987**.
3. Salaun, J. *Top. Curr. Chem.* **2000**, *207*, 1.

4. Faust, R. *Angew. Chem. Int. Ed,* **2001**, *40*, 2251.
5. Wessjohann, L. A.; Brandt, W. *Chem. Rev.* **2003**, *103*, 1625.
6. (a) Wang, G. W.; Gao, J. *Org. lett.*, **2009**, *11*, 2385. (b) Lebel, H.; Marcoux, J. F.; Molinaro, C.; Charette, A. B. *Chem. Rev.*, **2003**, *103*, 977. (c) Long, J.; Yuan, Y.; Shi, Y. *J. Am. Chem. Soc.*, **2003**, *125*, 13632. (d) Yang, D.; Gao, Q.; Lee, C. S.; Cheung, K. K. *Org. Lett.* **2002**, *4*, 3271. (e) Ni, A.; France, J. E.; Davies, H. M. L. *J. Org. Chem.*, **2006**, *71*, 5594. (f) Xu, Z. H.; Zhu, S. N.; Sun, X. L.; Tang, Y.; Dai, L. X. *Chem. Commun.* **2007**, 1960. (g) Hashimoto, T.; Naganawa, Y.; Kano, T.; Maruoka, K. *Chem. Commun.* **2007**, 5143. (h) Thompson, J. L.; Davies, H. M. L. *J. Am. Chem.* Soc. **2007**, *129*, 6090.
7. Nakanishi, K. *Natural Products Chemistry*, Kodansha Ltd., Academic, New York, **1974**.
8. Meyers, A. I. *Heterocycles in Organic Synthesis*, John Wiley & Sons, New York, **1974**, pp. 128-129.
9. Dean, F. M. *In Advances in Heterocyclic Chemistry*; (Ed. Katritzky, A. R.), Academic, New York, **1982**, *30*, 167.
10. Vernin, G. *The Chemistry of Heterocyclic FlaVoring and Aroma Compounds*; Ellis Horwood, Chichester, **1982**.
11. Danheiser, R. L.; Stoner, E. J.; Koyama, H.; Yamashita, D. S.; Klade, C. A. *J. Am. Chem. Soc.*, **1989**, *111*, 4407.
12. Fraga, B. M. *Nat. Prod. Rep.*, **1992**, *9*, 217.
13. Merrit, A. T.; Ley, S. V. *Nat. Pro. Rep.*, **1992**, *9*, 243.
14. (a) Mcdonald, F. E.; Connolly, C. B.; Gleason, M. M.; Towne, T. B.; Treiber, K. D. *J. Org. Chem.*, **1993**, *58*, 6952. (b) Pirrung, M. C.; Blume, F. *J. Org. Chem.* **1999**, *64*, 3642. (c) Lee, Y. R.; Suk, J. Y. *Tetrahedron.*, **2002**, *58*, 2359. (d) Lee, Y. R.; Hwang, J. C. *Eur J. Org. Chem.*, **2005**, 1568. (e) Hwu, J. R.; Chen, C. N.; Shiao, S. S. *J. Org. Chem.* **1995**, *60*, 856. (f) Nishino, H.; Nguyen, V. H.; Yoshinaga, S.; Kurosawa, K. *J. Org. Chem.*, **1996**, *61*, 8264. (g) Garzino, F.; Meou, A.; Brun, P. *Tetrahedron Lett.*, **2000**, 41, 9803. (h) Burgaz, E. V.; Yilmaz, M.; Pekel, A. T.; Oktemer, A *Tetrahedron* **2007**, *63*, 7229. (i) Wang, G. W.; Dong, Y. W.; Wu, P.; Yuan, T. T.; Shen, Y. B. *J. Org. Chem.*, **2008**, *73*, 7088.

15. Gennari, C.; Todeschini, R.; Beretta, M. G.; Favini, G.; Scolastico, C. *J. Org. Chem.* **1986**, *51*, 612.
16. Bouillon, J.-P. ; Portella, C.; Bouquant, J.; Humbel, S. *J. Org. Chem.* **2000**, *65*, 5823.
17. Arno, M.; Domingo, L. R. *Theor. Chem. Acc.*, **2002**, *108*, 232.
18. Zardoost, M. R. *Russ. J. Phys. Chem. B.*, **2013**, *7*, 540.
19. Liu, J.; Yang, Z.; Wang, Z.; Wang, F.; Chen, X.; Liu, X.; Feng, X.; Su, Z.; Hu, C. *J. Am. Chem. Soc.*, **2008**, *130*, 5654.
20. Fu, A.; Zhao, C.; Li, H.; Tian, F.; Yuan, S.; Duan, Y.; Wang, Z.; *J. Phys. Chem.* A., **2013**, *117*, 2862.
21. Polo, V.; Grafenstein, J.; Kraka, E.; Cremer, D. *Theor. Chem. Acc.*, **2003**, *109*, 22.
22. Johnson, B. G.; Gonzales, C. A.; Gill, P. M. W.; Pople, J. A. *Chem. Phys. Lett.*, **1994**, *221*, 100.
23. Eriksson, L. A.; Kryachko, E. S.; Nguyen, M. T. *Int. J. Quantum. Chem.* **2004**, *99*, 841.
24. Yang, W.; Morteir, W. J. *J. Am. Chem. Soc.*, **1986**, *108*, 5708.
25. Vos, A. M.; Schoonheydt, R. A.; Proft, F. D.; Geerling, P. *J. Catal.*, **2003**, *220*, 333.
26. Chattaraj, P. K.; Maiti, B. ; Sarkar, U. *J. Phys. Chem.* A., **2003**, *107*, 4973.
27. Fukui, K.; Yonezawa, T.; Shingu, H. *J. Chem. Phys.*, **1952**, *20*, 722.
28. Parr, R. G.; Yang, W. *J. Am. Chem.* Soc., **1984**, *106*, 4049.
29. Yang, W.; Mortier, W. J. *J. Am. Chem.* Soc., **1986**, *108*, 5708 .
30. Morao, I.; Cossio, F. *J. Org. Chem.*, **1999**, *64*, 1868.
31. Jiao, H.; Schleyer, P. V. R. *J. Phys. Org. Chem.*, **1998**, *11*, 655.
32. Gonzalez-Navarrete, P.; Coto, P. B.; Polo, V. Andres, J. *Phys. Chem. Chem. Phys.*, **2009**, *11*, 7189.
33. Pena-Gallego, A.; Rodriguez-Otero, J.; Cabaleiro-Lago, E. M. *Tetrahedron.*, **2007**, *63*, 11617.
34. Poater, A.; Ribas, X.; Liobet, A.; Cavallo, L.; Sola. M. *J. Am. Chem. Soc.*, **2008**, *130*, 17710.
35. Frisch, M. J.; Trucks, G. W.; Schlegel, H. B.; Scuseria, G. E.; Robb, M. A.;

Cheeseman, J. R.; Montgomery, J.; Vreven, Jr. T.; Kudin, K. N.; Burant, J. C.; Millam, J. M.; Iyengar, S. S.; Tomasi, J.; Barone, V.; Mennucci, B.; Cossi, M.; Scalmani, G.; Rega, N.; Petersson, G. A.; Nakatsuji, H.; Hada, M.; Ehara, M.; Toyota, K.; Fukuda, R.; Hasegawa, J.; Ishida, M.; Nakajima, T.; Honda, Y.; Kitao, O.; Nakai, H.; Klene, M.; Li, X.; Knox, J. E.; Hratchian, H. P.; Cross, J. B.; Adamo, C.; Jaramillo, J.; Gomperts, R.; Stratmann, R. E.; Yazyev, O.; Austin, A. J.; Cammi, R.; Pomelli, C.; Ochterski, J. W.; Ayala, P. Y.; Morokuma, K.; Voth, G. A.; Salvador, P.; Dannenberg, J. J.; Zakrzewski, V. G.; Dapprich, S.; Daniels, A. D.; Strain, M. C.; Farkas, O.; Malick, D. K.; Rabuck, A. D.; Raghavachari, K.; Foresman, J. B.; Ortiz, J. V.; Cui, Q.; Baboul, A. G.; Clifford, S.; Cioslowski, J.; Stefanov, B. B.; Liu, G.; Liashenko, A.; Piskorz, P.; Komaromi, I.; Martin, R. L.; Fox, D. J.; Keith, T.; Al-Laham, M. A.; Peng, C. Y.; Nanayakkara, A.; Challacombe, M.; Gill, P. M. W.; Johnson, B.; Chen, W.; Wong, M. W.; Gonzalez, C. and Pople, J. A. Gaussian 03, Revision D.01, Gaussian, Inc., Wallingford, CT, **2004**.